Failure of Welded Moment-Resisting Connections

ANDREW SHORT, WOLFRAM WOERNER, W. GEORGE FERGUSON, and G. CHARLES CLIFTON

When welds in moment-resisting connections (MRCs) are subject to seismic loads, they are generally designed and therefore expected to be stronger than the beam and column (Feeney and Clifton, 1995). Fractures observed in the welds of MRCs due to Northridge and Kobe earthquakes have challenged some long-held assumptions regarding the nature of stress and strain in the connection region (Goel, Stojadinovic, Choi, and Lee, 2000; Lee, Goel, and Stojadonovic, 2000; Plumier, 2000) and material response to cyclic inelastic strains (Kuwamura, 1997; Hyland, Ferguson, and Butterworth, 2003).

Achieving predictable and acceptable failure modes in large-scale tests is an important step in developing confidence in connection performance. As such, beam instability in the plastic hinge region has been described as the most common desirable ductile failure mode for post-Northridge connections (Stojadinovic, 2003). The two other modes observed in United States prequalification tests were lateral-torsional buckling of the column or entire connection subassembly, and "low-cycle connection fatigue" (Stojadinovic, 2003). Similar failure modes are seen in New Zealand large-scale tests. Low-cycle connection fatigue is expressed in this paper as cyclic ductile overload, reflecting the mechanism responsible for failure.

Acceptable failure modes are ones that allow the required ductility demands to be dependably resisted. Beam plastic hinging is the preferred failure mode; as with suitable beam geometry and material properties, this mode of failure can develop high cumulative plastic rotations. Lateral-torsional buckling of the assemblage can readily be suppressed through appropriate restraints; seismic codes have provisions for this [in other words, clause 12.6 in NZS 3404 (NZS, 1997)]. Cyclic ductile overload may or may not be an acceptable failure mode; it depends on the cumulative inelastic rotation capacity that can be developed before failure.

A number of parameters are known to influence the development of these failure modes. For example, weld imperfections act as stress-strain concentrators and subsequent initiation points for cyclic ductile overload of the connection weld. As such, the effect of volumetric imperfections on the integrity of connection welds is the first limiting case investigated. To date there have been relatively few large-scale model tests used in this research.

Increasing the resistance to shear deformation in the panel zone of moment-resisting connections (MRCs) during seismic loading is considered to provide enhanced weld performance (Mao, Ricles, and Fisher, 2001). With an adequate notch-tough weld metal, smooth connection geometry, and a strong panel zone, brittle and ductile weld fracture is suppressed, and the beam/column assemblage is therefore likely to fail because of beam plastic hinging, with flange and web buckling. The performance of specimens exhibiting this failure mode is limited by the reduction in resistance associated with buckling in the beams and panel zone such that for MRCs with very strong panel zones, the ductility of the connection is therefore limited by the inherent deformation capacity of the beam. This is the second limiting case investigated herein.

MRCs subject to seismic loads usually require butt welds (known in the United States as groove welds). The New Zealand structural steel standard NZS 3404 (NZS, 1997) in this instance permits the use of fillet welds. This paper therefore also provides preliminary evidence as to the acceptable performance of volumetric weld imperfections on the integrity of MRC fillet welds.

Following is an overview of the significance of imperfections and panel zones on connection performance and the test program conducted.

WELD IMPERFECTIONS

AS/NZS 1554.1 (AS/NZS, 2004), the structural steel welding code used in New Zealand and Australia, specifies im-

Andrew Short is a welding engineer, Auckland, New Zealand.

Wolfram Woerner is the manager, New Zealand Welding Centre, Heavy Engineering Research Association, Auckland, New Zealand.

W. George Ferguson is a professor, Department of Chemical and Materials Engineering, University of Auckland, Auckland, New Zealand.

G. Charles Clifton is the senior structural engineer, Structural Division, Heavy Engineering Research Association, Auckland, New Zealand.

perfection acceptance based on imperfection dimensions and location. As reflected in these provisions, embedded imperfections are, in general, less detrimental to performance than surface imperfections (Mohr, 2002). An alternative acceptance-rejection criterion to the ultrasonic size-based criterion in AWS D1.1 (AWS, 2004) has been proposed by Mohr (Johnson, 2000; Mohr, 2002). Based on a brittle failure mode, a depth of less than 3 mm is proposed for surface or near surface imperfections and less than 6 mm for embedded imperfections.

There are also specific requirements with regard to imperfection area due to a distinction between brittle and ductile modes of fracture. Brittle initiation is regarded as sensitive to the height of the imperfection, while ductile initiation is sensitive to imperfection area (Johnson, 2000). Different rules are used for characterizing imperfections in engineering critical assessments (ECA) methods depending on the likely failure mode (Phaal, Challenger, Maddox, and Garwood, 1995).

Furthermore, the type of load has an affect on the permissible imperfection limits. A comparison of permissible imperfection sizes to New Zealand standards demonstrates that welds subject to seismic loading [structural purpose category (SP) in AS/NZS 1554.1 (AS/NZS, 2004)] are less affected by imperfections than welds subject to high levels of fatigue loading [fatigue purpose category (FP) in AS/NZS 1554.5 (AS/NZS, 1995)]. The latter scenario has more stringent requirements. With high levels of fatigue loading, surface imperfections detected by visual and magnetic particle inspection, except in reinforcement, and undersize welds are not permitted (AS/NZS, 1995). In comparison, AS/NZS1554.1 (AS/NZS, 2004) permits a variety of surface imperfections for welds subject to seismic loading. This effect is also established for subsurface imperfections such as lack of fusion and lack of penetration by the limits set within these standards.

Among specific requirements pertaining to individual imperfection types in AS/NZS1554.1 (AS/NZS, 2004), the maximum "loss of cross-sectional area" pertaining to a summation (or aggregate) of all allowable internal and surface imperfections (for example, inclusion, lack of fusion, undercut, and misalignment) is specified. This *imperfection level* is specific to the particular weld category and must be less than

5% for structural purpose (SP) welds
10% for general purpose (GP) welds

No cracks (including hot cracks, cold cracks, and crater cracks) are allowed in SP category welds. The imperfection level specified for butt and fillet welds are similar and assume that the parent metals and weld metals "have been selected to avoid the risk of brittle fracture" (AS/NZS, 2004). For weld consumables used in seismic applications, NZS 3404 (NZS, 1997) requires a minimum Charpy V-Notch (CVN) impact energy of 47 J at 0 °C.

PANEL ZONE DEFORMATION

The largest component of inelastic behavior for connections with panel zones weak in shear is developed by the deformation of the panel zone (Krawinkler and Mohasseb, 1987). In contrast, connections with panel zones that are strong in shear will experience deformation concentrated at the plastic hinge in the beam. This is generally also the failure mode.

Doubler plates or heavy column sections will be required to achieve a strong panel zone. A review of the use of column stiffening and design provisions including continuity plates and doubler plates is given elsewhere (Hajjar, Dexter, Lee, Cotton, Ye, and Ojard, 2003). As these methods may add significant cost to a structure, and because panel zone deformation may be used to help achieve ductility, design codes have increased the emphasis of utilizing weak panel zones (Roeder, 2000; Hajjar, 2003). Excessive panel zone deformation is, however, known to promote weld fracture (Krawinkler and Mohasseb, 1987; Mohr, 1997; Calado, Castiglioni, and Bernuzzi, 2000; Lu, Ricles, Mao, and Fisher, 2000; Plumier, 2000; Mao et al., 2001). Poor weld performance is due to "kinking" in the column flanges and the subsequent large inelastic stress and strain demands in the column flange region into which the beam-to-column flange connects (Krawinkler and Mohasseb, 1987; Plumier, 2000; Roeder, 2000).

As a method for reducing the likelihood of weld fracture, one may therefore consider significantly strengthening the panel zone. As such, a design imperative exists to optimize the contribution of the panel zone to overall deformation capacity against the increased likelihood of weld fracture. The relationship between panel zone yielding and total plastic rotation, θ_p, in MRCs with notch-tough filler metals has been investigated (Roeder, 2000; Roeder, 2002). The historic data show significant scatter. In spite of this, specimens with weak panel zones have been seen to develop smaller total plastic rotations, θ_p, than specimens with stronger panel zones (Roeder, 2002). This is also shown in the results from Task 7.05 of Phase 2 of the SAC* steel project where contributions to the total plastic rotation, θ_p, from the panel zone, column and beam were categorized (Ricles, Mao, Lu, and Fisher, 2002). It has been proposed that "the largest

*SAC is a partnership of Structural Engineers Association of California (SEAOC), Applied Technology Council (ATC), and California University for Research in Earthquake Engineering (CUREE).

Table 1. Overview of Tests				
	Configuration	**Weld Size**	**Panel Zone**	**Imperfection %**
BE18	Beam-End-Plate	Design Size	Rigid (End-Plate)	N/A
BE19	Beam-End-Plate	Smaller	Rigid (End-Plate)	N/A
BE20	Beam-End-Plate	Smaller	Rigid (End-Plate)	N/A
BC22	Beam-Column	Design Size	$0.94V_y$	5
BC27	Beam-Column	Design Size	$0.94V_y$	2.5
BC28	Beam-Column	Design Size	Hardened Panel Zone	2.5
BC29	Beam-Column	Design Size	Hardened Panel Zone	5
BC30	Beam-Column	Design Size	$0.94V_y$	10

rotational capacities occur for specimens that first yield in beam flexure but yield shortly thereafter in the panel zone" (Roeder, 2002). A balanced design condition to achieve this has been proposed (Roeder, 2002) such that

$$0.9V_y > V_{pzMy} > 0.6V_y$$

where

V_{pzMY} = panel zone shear

$$= \frac{\sum M_{cl}}{d_b} - V_c$$

M_{cl} = moment at the column centerline

V_c = column shear force

V_y = $0.6f_{yc}d_ct_{wc}$

The NZS 3404 (NZS, 1997) provisions for panel zone design recommend that the relationship is always set relatively high and therefore fall into the more conservative end of this criterion. These provisions are based on limiting the panel zone strain to less than 1% under severe earthquake demand. Using typical values for each category of member, the New Zealand criteria are $0.94V_y$ for Category 1 MRCs, $0.90V_y$ for Category 2 MRCs and $0.77V_y$ for Category 3 MRCs. Category 1 MRCs are fully ductile, Category 2 MRCs are limited ductile, and Category 3 MRCs are nominally ductile (NZS, 1997). The typical maximum magnitude of plastic rotation demand on the beams is 30 mrad, 15 mrad, and 5 mrad for Categories 1, 2, and 3 respectively.

OVERVIEW

The limits for fillet welds with worst-case volumetric imperfections and the deformation capacity of connections with strong panel zones designed to the New Zealand Category 1 MRCs are investigated. Five full-scale welded MRC specimens designed to New Zealand codes (NZS, 1997; AS/NZS, 2004), and three modified beam-end-plate specimens were subject to seismic deformation following ATC-24 (Krawinkler, 1992) (see Table 1).

Following is an overview of the design of the rigid welded connections and beam-end-plate specimens, and the design of the weld and weld imperfections.

DESIGN MODEL

Design of Rigid Welded Connections

A brief summary of the connection design is presented herein. The MRC specimens tested were based on typical beam-to-column connections in medium-sized moment-resisting frames according to New Zealand design provisions. The test specimens consisted of a 410 UB 54 beam (similar to W16×36) joined to a 460 UB 75 column (similar to W18×50); see Figures 1 and 2. Here, a sufficiently strong

Fig. 1. Beam-column test setup.

column was used to ensure that during cyclic loading, the beam can develop a plastic hinge before significant deformation or damage is developed in the column (Hyland, Clifton, Butterworth, and Scholz, 2000). This is achieved by designing the column for the overstrength actions from the beam. The tension and compression stiffeners are designed to transmit the internal axial forces from overstrength beam action, into the column via the flanges and web. Similarly, the panel zone design is based on inelastic actions occurring in the panel zone subsequent to the yield of the incoming beam. This is achieved by requiring the input beam moment to be the nominal section moment capacity of the beam multiplied by a factor that depends on the ductility demand of the system. This factor varies from 1.15 for Category 1 to 1.0 for Category 3. The panel zone is designed at the upper end of the United States' balanced design limits with the plastic panel zone design shear capacity taken from Equation 12.9.5.3(5) of NZS 3404 (NZS, 1997) [similar to Equation 2-3b in FEMA 355D (Roeder, 2000)] given as

$$\phi_p V_p = 0.54 f_{yc} d_c t_{wc} \eta \left(1 + \frac{3 b_c t_{cf}^{\,3}}{d_b d_c t_{wc}}\right) = 1.5 \text{ MN}$$

where

f_{yc} = column yield strength = 329 MPa
d_c = column depth of section = 457 mm
t_{wc} = column web thickness = 9.1 mm
b_c = column flange width = 190 mm
t_{cf} = column flange thickness = 14.5 mm
d_b = beam depth of section = 403 mm
η = column axial load reduction factor = 1.0 for these tests

Specimens BC28 and BC29 reuse the columns from BC22 and another specimen not reported here. Also, BC27 uses a built-up beam with geometry and material properties close to 410 UB 54. Here, a single weld is used to connect the flange to the web.

Modified Beam-End-Plate Specimen Test Configuration

The basic geometry for a beam-end-plate specimen is comparable to a beam-column specimen outlined above. The major difference between a beam-end-plate specimen and a MRC specimen is that the 410 UB 54 beam is mounted to an end-plate instead of a column. The end-plate is mounted to a 60-mm-thick steel plate, which was in turn mounted onto the reinforced concrete reaction wall. The steel plate was fixed to the wall by eight 25-mm-diameter Macalloy bars. The test setup is shown in Figures 3 and 4.

In this design, it is first assumed that no inelastic action would occur in the supports. This maximizes the inelastic rotational demand in the beam. Secondly, this design was

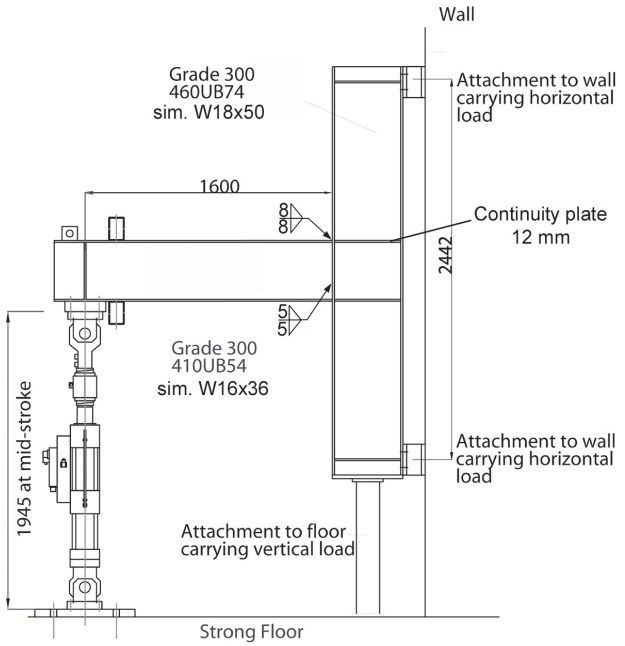

Fig. 2. Drawing of the beam-column test setup.

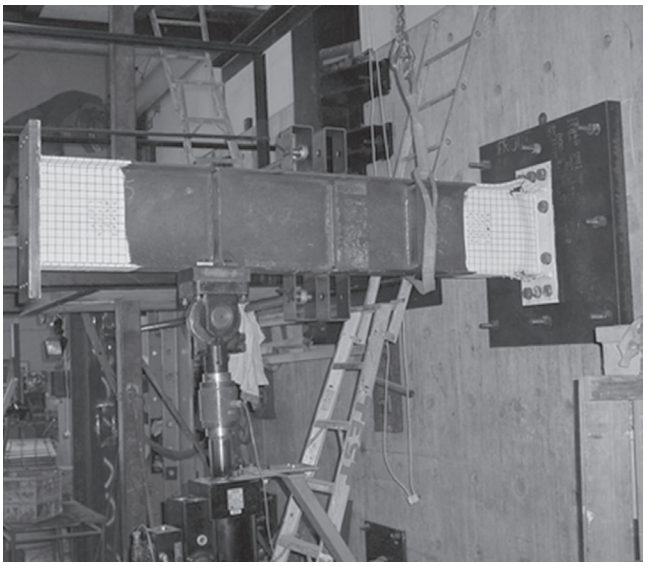

Fig. 3. Photograph of the beam-end-plate test setup.

based on the stiffness in the supports being at least as great as that in the beam-column.

Weld Design

A thorough review of weld size formulation and the design of the beam web to column flange fillet weld is found elsewhere (Short, Woerner, Vogele, and Moll, 2004). The *stress component method*, based on the von Mises failure criterion is used to design the double-sided and balanced fillet welds. A basic development for the throat thickness of the flange weld is given as follows:

$$v_w^* \le \phi v_w$$

$$v_w = 0.6 f_{uw} t_{tf} k_r \left(\sqrt{3}/\sqrt{2}\right)^*$$

$$v_w^* = \frac{\phi_{oms} b_f t_{fb} f_y}{L_w}$$

$$t_{tf} \ge \frac{\sqrt{2}\phi_{oms} b_f t_{fb} f_y}{\sqrt{3}\phi 0.6 f_{uw} L_w}$$

where

v_w^* = capacity of fillet weld per unit length

v_w = nominal capacity of fillet weld per unit length

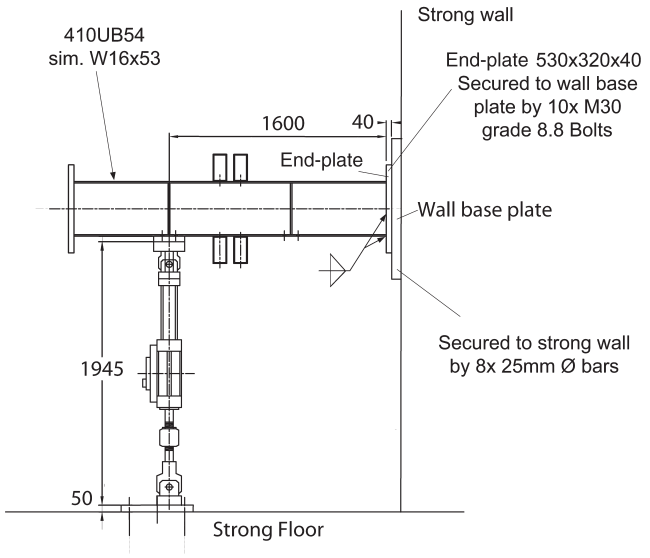

Fig. 4. Drawing of the beam-end-plate test setup.

ϕ = strength reduction factor for weld according to NZS 3404 (1997); for fillet weld, Category SP = 0.8

f_{uw} = the nominal tensile strength of the weld metal = 480 MPa

t_{tf} = design throat thickness of flange weld = $t_w/\sqrt{2}$ for an equal leg length fillet weld

k_r = reduction factor [given in Table 9.7.3.10(2) NZS 3404: Part 1:1997] to account for the length of a welded lap connection = 1.0 for these tests

ϕ_{oms} = overstrength factor according to NZS 3404 (1997), incorporating statistical variation in yield stress and a strain hardening component; for the material employed, ϕ_{oms} = 1.25

b_f = width of the beam flange = 178 mm

t_{fb} = thickness of beam flange = 10.9 mm

t_{wb} = thickness of beam web = 7.6 mm

f_y = nominal yield strength of the incoming beam material = 310 MPa

L_w = length of weld = $2b_f - t_{wb}$

$\sqrt{3}/\sqrt{2}^*$ = factor due to resolving the stress on a plane (the throat) at 45° to the incoming beam

The design size for the weld is compared to the measured size in Table 2. Unlike the full strength scenario found in BE18, BC22 and BC27-BC30, the welds in specimens BE19-BE20 were reduced in size by changing the design safety factors (see Table 2). This was to find the minimum weld size for preferential failure due to inadequate weld cross-sectional area, and not beam plastic hinging. The design throat thickness of beam web to column flange fillet weld, t_{tw}, is also given.

Imperfection Shape, Location, and Size

A series of imperfections were designed for each of the beam-column specimens BC22 and BC27–30. An imperfection dimension based on a "loss in cross-section" of the total welds in one flange was used as the imperfection variable to simplify test requirements. This imperfection may be compared to loss of cross-section imperfections such as lack of fusion, undercut, and linear misalignment. The single variable was chosen because it may be considered the most severe scenario when all allowable internal and surface imperfections are aggregated at a single location.

As discussed earlier, brittle fracture initiation is regarded as being sensitive to imperfection height and ductile fracture initiation sensitive to imperfection area. Furthermore, surface breaking imperfections will induce considerably higher stress concentrations. The imperfection was therefore designed such that it had the full weld height at the investigated imperfection area and was surface breaking.

Table 2. Overview of Weld Sizes						
Test	Weld Design Factors		Beam Flange-to-Column Flange Weld, mm		Beam Web-to-Column Flange Weld, mm	
	ϕ	ϕ_{oms}	Design, t_{tf}	Measured	Design, t_{tw}	Measured
BE18	0.8	1.25	8.0	7.3 ± 1.0	5.0	7.0 ± 1.4
BE19	1	1	5.0	4.2 ± 0.3	4.0	3.2 ± 0.2
BE20	1.4	1	4.0	3.3 ± 0.3	3.0	2.9 ± 0.2
BC22	0.8	1.25	8.0	8.8 ± 0.8	5.0	5.0 ± 0.0
BC27	0.8	1.25	8.0	9.3 ± 0.6	5.0	5.0 ± 0.0
BC28	0.8	1.25	8.0	8.6 ± 1.3	5.0	5.0 ± 0.0
BC29	0.8	1.25	8.0	8.7 ± 0.4	5.0	5.0 ± 0.0
BC30	0.8	1.25	8.0	8.6 ± 0.5	5.0	4.8 ± 0.4

Table 3. Dimensions of Artificial Imperfections						
Specimen	Designed Imperfection		Measured Dimensions			
			d_1	d_2	d_3	d_4
	%	mm	mm			
BC22	5	17.8	Not det.	18.5	2.5	18
BC27	2.5	8.9	Not det.	8.5	0	8
BC28	2.5	8.9	91	10	–2	9
BC29	5	17.8	86	17.5	0	21
BC30	10	35.6	73	36	–7	35

The artificial imperfection size based on a loss in load bearing cross-section was varied in size from 2.5% to 10%, as shown in Table 3. The weld imperfection size was based on the weld area connecting a single beam flange to column, as this comprises one element of weld. In practice, a 2.5% loss of area imperfection would fail the individual imperfection limits specified in AS/NZS 1554.1 (AS/NZS, 2004) as a lack of fusion imperfection is not allowed to have a length of more than 2*t*/3 (in this case 7.3 mm) when located more than 3*t* from the edge of a weld or 3 mm when located within 3*t*.

The location of the imperfection has a significant bearing on weld performance (Barsom and Pellegrino, 2002). Therefore, two different positions in the weld were selected. On the bottom flange, the imperfection was placed at the flange edge, while on the top flange the imperfection was placed midwidth (see Table 3 and Figure 5). The symmetrical demand on the beam and the joint permitted the testing of both configurations at the same time. Of the two fillet welds that are used to join each beam flange, the outside fillet welds to this flange are considered to be more severely loaded. The imperfections were subsequently located in these welds.

In order to accurately generate welding imperfections of a specific size, unfused regions were specifically constructed. In Specimen BC22, steel blocks were introduced into the welds (see Figure 6). This method was similar to that used by Azuma, Kurobane, and Makino (2000) in partial-joint-penetration (PJP) groove welds. The imperfections in specimens BC27–BC30 were created by removing weld metal with a pencil grinder (see Figure 7). All welds outside of the artificial imperfection complied with all of the imperfection limits for SP welds.

Material Properties

The hot-rolled 410 UB 54 beams and the 460 UB 75 columns were made according to AS 3679.1-300. The mechanical properties of the beam given in Table 4 are the average values from two tensile coupons located at the edge and midwidth of the flange. The mechanical and chemical properties for the column given in Table 4 are from the mill certificate. Steel, made in New Zealand to this standard, have been shown to have excellent CVN temperature transition curve characteristics, featuring a subzero 27 J transition temperature, a steep transition range, and high upper-shelf energy (over 120 J at 0 ºC) (Hyland, Ferguson, and Butterworth, 2004).

Two welding processes were used in the tests. Specimens BE18–BE20, BC22, BC27, and BC28 were made using GMAW process with E70s-6 electrodes. Specimens BC29 and BC30 were made using MMAW process with E6013 electrodes. Both materials show excellent notch-tough properties; with the mechanical and chemical properties given in Table 5.

EXPERIMENTAL PROCEDURE

Instrumentation

The force and displacement of the actuator were measured. Additional measurements of the average shear deformation in the panel zone and strain at the outside surface of the bottom beam flange were taken for Specimens BC27–BC30. The shear deformation was measured across the continuity plates using portal gauges.

Cyclic Loading Systems

The beam-to-column tests were conducted at the University of Auckland. A remote MTS servo-controlled, closed-loop, hydraulic actuator mounted on a swivel base was used to supply the load regime to the specimen. The system is rated to deliver ±320 kN with a stroke of ±100 mm.

Loading History

The loading history for testing the specimens was developed based on the guidelines developed for cyclic seismic testing of components of steel structures in ATC 24:1992 (Krawinkler, 1992) but with some alterations. This guideline recommends a stepwise increase of deformation cycles with a minimum of at least three cycles at each deformation step.

The specimens were loaded at dynamic rates, with deformation control. A deformation control parameter, Δ, derived later, was used as the increment in deformation between two steps. The loading history consists of a stepwise increase of deformation cycles with three cycles at 0.75Δ, 1Δ, and 2Δ and extended cycles until failure at 3Δ (see Figure 8). A monotonic force controlled step was used to calibrate the specimen and estimate δ_y. The yield deflection, δ_y, is used as

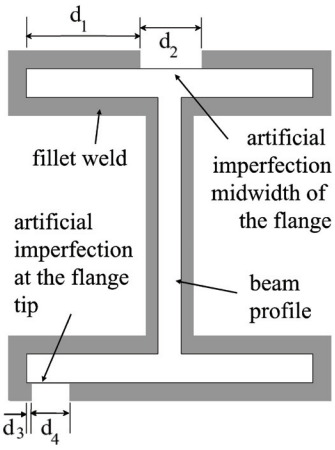

Fig. 5. Location of the artificial imperfections.

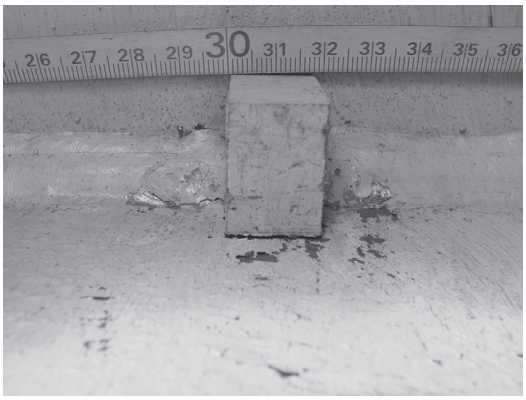

Fig. 6. Midwidth imperfection simulated by a steel block in BC22.

Fig. 7. Flange edge imperfection simulated by removing weld metal in BC29.

Table 4. Beam and Column Mechanical and Chemical Properties									
Material	**C %**	**Mn %**	**Si %**	**P %**	**S %**	**Al %**	**f_y MPa**	**f_u MPa**	**Elongation in 50 mm**
Beam	0.16	0.90	0.27	0.02	0.03	0.01	373	517	36
Column	0.15	0.70	0.21	0.02	0.03	< 0.01	329	485	27

Table 5. Weld Metal Mechanical and Chemical Properties											
Material	**C %**	**Mn %**	**Si %**	**P %**	**S %**	**Al %**	**f_y MPa**	**f_u MPa**	**Elongation in 50 mm %**	**Charpy Impact Values at 20 °C J**	**Average Impact Value J**
MMAW	0.09	0.43	0.29	0.03	0.009	< 0.001	449	487	29	110/98/110	106
GMAW	0.06	1.13	0.66	0.01	0.022	0.003	472	566	25	129/137/136	134

the deformation control parameter, Δ (see Calibration Tests below).

The frequency and loading rate were determined so that at the 3Δ step, they corresponded with that typically expected for severe earthquakes in a medium-rise building undergoing inelastic deformation, namely, 1 cycle per second (Clifton, Weigel, and Rupflin, 1996; Clifton and Butterworth, 1998). The loading rate for all tests was 150 mm/s. This entails a reduction in frequency as the test progresses.

Calibration Tests

The yield deflection (δ_y) is used as the deformation control parameter, Δ. Design of the test setup configuration predicted yield to first occur in the beam at the column face. For the beam-column (BC) specimens, yield was calculated from the beam section moment capacity (386 kN-m). This was calculated as $Z_e f_{y,act}$, where Z_e is the plastic section modulus of the nominal cross-section and $f_{y,act}$ is the actual yield stress. As the deflection was approximately linear prior to yield, the configuration was loaded to 75% of calculated yield force. The deflection was measured at the actuator and subsequently converted to 100%, giving the yield deflection, δ_y.

Unlike the calibration tests for the beam-column specimens, a destructive monotonic bend test was used to establish the mechanical properties of the beam-end-plate (BE) configurations. Based on the results of this test, δ_y for the subsequent beam-end-plate tests (BE18–BE20) was determined to be 25.6 mm. The maximum monotonic bending strength of the 410 UB 54 beam-end-plate specimen was 265.7 kN at 53.3 mm displacement.

Instrumentation of the Panel Zone

The panel zone shear rotation was approximated by measuring four displacements across the panel zone as shown in

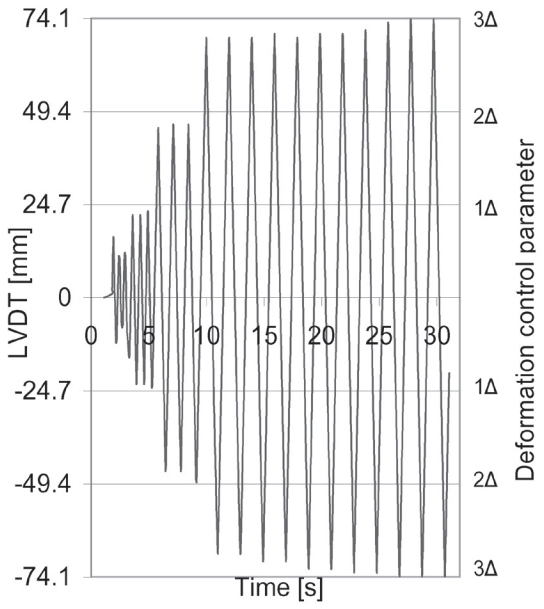

Fig. 8. Displacement achieved at actuator for BC27.

Table 6. Overview of Test Results										
Test	Δ mm	F_{max} kN	Cycles to Failure, N_f	ED kJ	Failure Mode	Designed Imperfection %	Cycles to Buckle, $N_{i,p}$	Cycles to Crack Initiation, $N_{i,c}$	Test Temp. °C	Mean Flange Temp. Post Test °C
BE18	25.6	–291	4@3Δ	201	BPH	N/A	Not Det.	N/A	Not Det.	Not Det.
BE19	25.6	–300	4@3Δ	276	BPH	N/A	2¾ @ 1Δ	N/A	19.3	47.3 ± 20.0
BE20	25.6	303	4@3Δ	237	BPH	N/A	2¼ @ 1Δ	N/A	21	54.8 ± 34.9
BC22	18.8	281	9@3Δ	354	CDO	5	4¾ @ 3Δ	3¼ @ 3Δ	22.5	Not Det.
BC27	24.7	288	8@3Δ	435	BPH	2.5	2¼ @ 2Δ	N/A	18	47.2 ± 14.1
BC28	24.3	289	3@3Δ	194	BPH	2.5	2¼ @ 2Δ	N/A	22	72.6 ± 21.6
BC29	24.3	292	3@3Δ	127	BPH	5	2¼ @ 2Δ	N/A	20	55.3 ± 22.7
BC30	24.3	280	3@3Δ	190	CDO	10	1¾ @ 3Δ	2¼ @ 3Δ	21	36.2 ± 6.0

BPH = beam plastic hinging
CDO = cyclic dutile overload
ED = energy dissipated

Figure 9. This was only measured for BC27–BC30, as analysis of previous results and literature provided evidence that the performance of the panel zone influenced the demand at the weld. The displacements were measured with portal transducers with the results recorded on the TestWare-SX™ program. The recorded movement between the flanges of the column and the strong wall was converted to a measure of panel zone rotation in the following manner.

$$\theta_p = \frac{(A+0.5B)-(C+0.5D)}{d_c}$$

where

d_c = depth of the column
θ_p = panel zone rotation in shear
A, B, C, and D = recorded displacements as shown in Figure 9

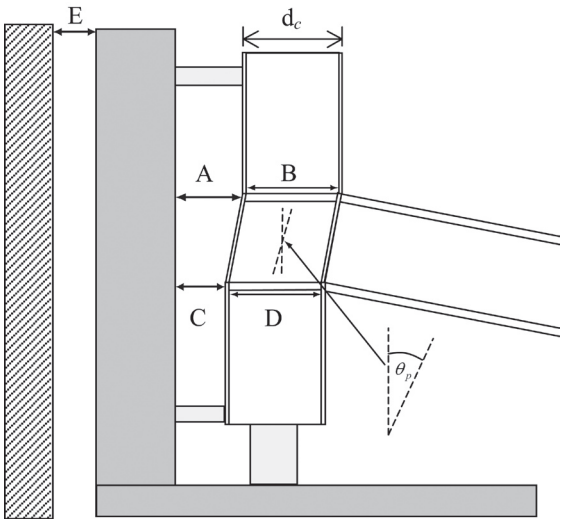

Fig. 9. Instrumentation of tests.

RESULTS

Calibration

The predicted yield force, Q_y, for the beam was shown to be similar to the measured Q_y in the monotonic bend test. The beam-end-plate tests were subject to larger Δ than that used in the beam-column tests.

Specimen Performance

The specimens were categorized to fail by either cyclic ductile overload (CDO in Table 6) of the material in the connection region, or beam plastic hinging (BPH in Table 6) dependent on fracture mode (also see Figures 10 through 13). None of the specimens tested failed due to brittle fracture.

The number of cycles to failure, N_f, was determined as the last complete cycle before the specimen resistance reduced to 80% of the maximum resistance achieved within

an individual deformation step, as defined by the loadings standard (NZS, 1992). In all specimens, final fracture occurs well after the specimen has failed by the above criterion (see Figures 12 and 13). Three cycles at 3Δ corresponds to a plastic hinge rotation (θ_p) of approximately 45 mrad. From comparison to NZS 3404:1997 (NZS, 1997) Table 4.7(1), this is satisfactory to classify the beam to Category 1 (fully ductile) response.

The energy dissipated (ED in Table 6) is calculated from the area inside the force-displacement hysteresis at failure. Cycles to buckle, $N_{i,p}$, and cycles to crack initiation, $N_{i,c}$, are qualitative measurements assessed from video footage. The temperature of the flange was measured post-test at six points. The increase in temperature is due to the plastic deformation occurring at dynamic rates.

The three beam-end-plate specimens (BE18–BE20) all failed due to beam plastic hinging after enduring four cycles at 3Δ (BPH in Table 6). The force-deflection relationships reveal a consistent degradation in strength in all specimens. Due to the lack of weld failure in BE18 and then BE19, the design throat thickness was reduced to be significantly undersize (see Table 2). The final specimen in this series, BE20, had the fillet weld throat in the beam flange reduced to 3.5 mm by mechanical grinding.

The five beam-column specimens (BC22 and BC27–30) failed with both beam plastic hinging and cyclic ductile overload, after enduring a minimum of three cycles at 3Δ (Table 6). Where the specimen failed due to cyclic ductile overload, the crack initiated adjacent to the flange edge imperfection. These cracks were seen to propagate in a stable manner for a number of cycles to a critical size. At this point, rapid propagation of the crack (catastrophic failure) occurred (see Figure 13). The specimen invariably failed due to a loss in resistance before the crack reached this critical size. Cracks were also observed to initiate at many midwidth imperfections, but this did not progress to failure.

Panel Zone Deformation

All MRC tests exhibited significant column panel zone deformation except the already tested (hardened panel zone) specimens BC28 and BC29. In these tests, the panel zone deformation was not large enough to flake the whitewash paint. All panel zones maintained their at-rest shape and did not undergo local buckling. From analysis of the recorded panel zone performance, a variety of deformation patterns are evident in nominally identical zones. The measured maximum and minimum panel zone rotation is presented in Table 7. Panel zone rotation hystereses (see Figure 14) were seen to be asymmetric. Specimens BC27 and BC28 were seen to develop a shift in the center of rotation.

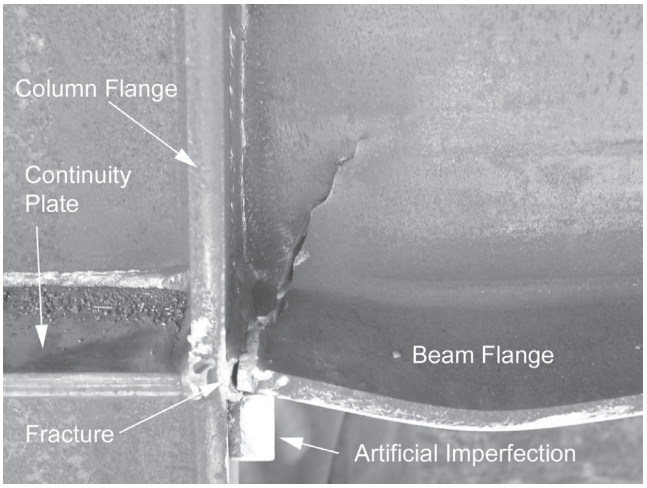

Fig. 10. Failure by cyclic ductile overload in specimen BC22.

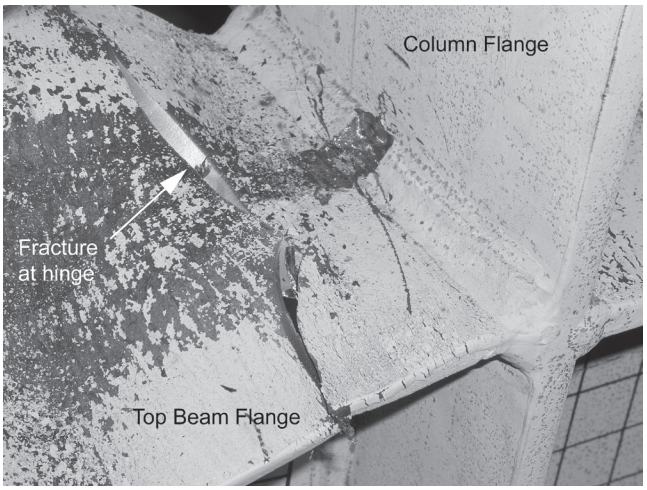

Fig. 11. Failure by beam plastic hinging in specimen BC29.

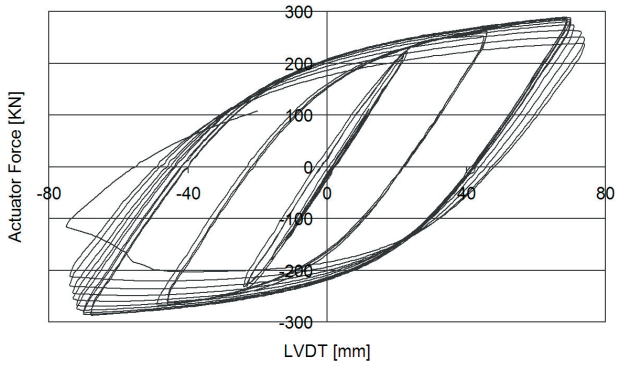

Fig. 12. Force-displacement hysteresis for T27.

Table 7. Overview of Maximum and Minimum Panel Zone Rotation				
Specimen	BC27	BC28	BC29	BC30
Max. Rotation (mrad)	1.09	0.72	0.64	0.95
Min. Rotation (mrad)	–1.34	–0.56	–0.58	–0.96

DISCUSSION

Achieving predictable and acceptable failure modes in large-scale tests is an important step in developing confidence in connection performance. Cyclic ductile overload may or may not be an acceptable failure mode. It may be argued to be acceptable given a dependable and sufficient cumulative inelastic rotation capacity.

Volumetric Imperfections

Critical volumetric imperfection parameters have been determined for the minimum required deformation capacity of a connection and the threshold between desirable, beam plastic hinging and undesirable, cyclic ductile overload, failure mechanisms. Failure by cyclic ductile overload of the weldment is induced by the size and location of the imperfection.

If cyclic ductile overload of the weldment is an acceptable limit state, a reduction in the load-bearing cross-section of the fillet weld by 10% flange-edge volumetric imperfection was shown to provide marginally acceptable deformation capacity (three cycles at 3Δ) and a relatively fast ductile failure. This specimen (BC30) employed the standard panel zone stiffness and the imperfection two times larger than allowed by the aggregate clause (AS/NZS, 2004).

Volumetric imperfections above a threshold value in the beam flange fillet welds were shown to change the failure mode from beam plastic hinging to cyclic ductile overload of the weldment. A threshold based on the size of an imperfection positioned at the flange-edge of the beam was determined. Specimens with 5% "loss in cross-section" imperfections at the beam flange edge were seen to fail with both beam plastic hinging and cyclic ductile overload. These specimens (BC22 and BC29) differ in both panel zone strength and deformation control parameter, Δ. The failure due to beam plastic hinging (BC29) is attributed to a hardened panel zone as consideration of the force against time curves demonstrated that the joints were subject to similar forces. Where the specimen failed with cyclic ductile overload (BC22), fracture initiated adjacent to the flange edge imperfection. This indicates that for MRCs with typical panel zones, the stress concentration due to a 5% imperfection was large enough for the cyclic crack growth to dominate among competing failure mechanisms and the failure mode change from beam plastic hinging to cyclic ductile overload. Additional evidence has been given elsewhere (Short et al., 2004). Other results reported confirm this threshold, as specimens with 2.5% imperfections were seen to fail due to

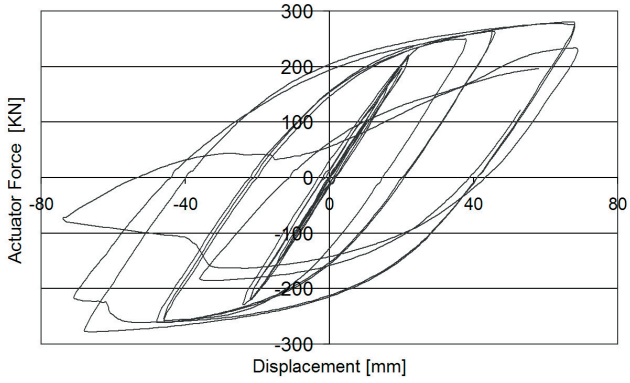

Fig. 13. Force-displacement hysteresis for T30.

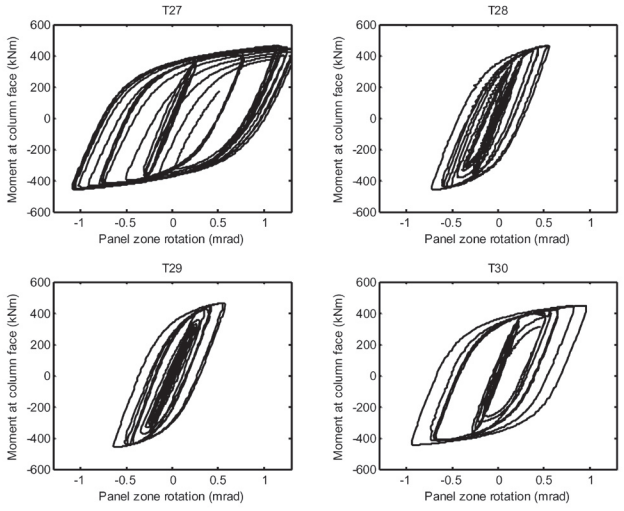

Fig. 14. Comparison of panel zone rotation for BC27–BC30.

beam plastic hinging and specimens with 10% imperfections seen to fail due to cyclic ductile overload.

The flange edge volumetric imperfections simulate the worst-case scenario for an aggregate of imperfections following permissible levels for a loss in cross-section to AS/NZS (2004). As mentioned before, the simulated imperfections are greater than specified for an individual lack of fusion imperfection as specified in this standard, and in U.S. specifications (Johnson, 2000; Mohr, 2002). This indicates that the permissible imperfection levels as related to seismic performance of MRCs are relatively conservative and reflect workmanship rather than performance requirements.

Beam Buckling and Weld Fracture

Local buckling of the beam must be considered in the assessment of weld imperfections. This is because buckling decreases the load transmitted through the weld, the deformation in the panel zone, and the subsequent stress/strain state at imperfections in the weld. A comparison of tests subject to different deformation control parameters, Δ (for example, BC22 and BC30), demonstrates that specimens subject to large Δ develop beam buckling earlier in the loading regime, due to increased ductility demand at 2Δ and 3Δ cycles that will occur where the support is relatively flexible, thus increasing Δ. This value is governed by elastic deflection, so all components contribute to Δ. However, the subsequent cycles to 2Δ and 3Δ all require plastic rotation of the beam, so the larger Δ, the greater the plastic rotation in subsequent cycles.

Some scatter in the initiation was also evident (see Table 6). With the onset of local buckling, the force required to achieve the deformation demanded by the control system generally decreases as the beam section moment capacity decreases. In general, this reduction does not occur at the onset of flange buckling, but only once web buckling also occurs.

As outlined earlier, the connection is considered to have failed due to beam plastic hinging when the beam strength is reduced below 80% of the maximum strength achieved due to buckling effects (NZS, 1992). The following discussion is based on behavior of the assembly after this criterion is realized. If a crack in the weld has not reached a sufficient size at this point, further propagation is unlikely. The weld is protected, as the stress at the crack tip will decrease as the force decreases. An increase in stress is a fundamental requirement for further ductile propagation (Lange, 1986), which means that once the specimen has failed due to the formation of a plastic hinge, weld fracture is unlikely. However, this does not mean that a specimen is protected from cyclic ductile overload by the initiation of buckling, as generally it takes several cycles after the initiation of buckling before a reduction in strength is noticed. This course of action has been observed in specimen BC30, which failed with cyclic ductile overload but also developed buckling in the beam flanges.

Local buckling may also induce a more severe state of stress in the weld at the flange edge weld toe as the weld is put into bending. This is due to the straightening of the beam flange required to transfer the force into the column.

Support Deformation and Weld Fracture

Panel zone deformation is considered to be a significant indicator of the demand placed on weld imperfections. Rigid backing as provided by the beam-end-plate configuration (BE18, BE19, and BE20) and strong panel zones of BC28 and BC29 provide protection of the weld metal adjacent to the fillet weld imperfection as it is subject to smaller strains. This is evident with comparison of BC22 and BC29 as discussed earlier. Furthermore, a comparison of panel zone rotation demonstrates that Specimens BC28 and BC29 exhibit approximately 50% of the panel zone rotation measured in BC27 and BC30 (see Table 7 and Figure 14).

Additional support for this outcome is also found with a force degradation comparison to that observed in the beam-end-plate tests. Here similar protection was observed in the case of significantly undersize welds (BE19–BE20). It is proposed that the beam-end-plate specimens transfer more of the load through the web. Furthermore, published beam-end-plate tests (Woerner, Mago, Schwarz, and Short, 2003) with 10% flange-edge imperfection did not induce cyclic ductile overload of the weld as observed in the beam-column test of BC30. The threshold where the failure mode changes from beam plastic hinging to cyclic ductile overload of the weldment in beam-end-plate specimens was shown to be larger than the 5% determined for the beam-column tests. In these investigations, beam-end-plate specimens subject to 15% and 20% flange edge imperfections failed with ductile overload.

As the focus of this research did not initially address a range of panel zone provisions, the specimens tested were designed in accordance with New Zealand provisions; that is, at the higher strength limits of U.S. recommendations. The discussion on the influence of volumetric imperfections is valid for the range of panel zone strengths tested. Quite possibly, if the panel zone strength were much reduced, then secondary stresses in the column adjacent to the weld face would be greater and subsequently have a greater influence on the weld. Subsequently, a control of defect limits is more critical. This is unfortunately outside the scope of this research.

Specimen Performance

The test procedure employed the stepwise increasing loading regime recommended in ATC-24 (Krawinkler, 1992). Following this loading regime, all specimens were shown to endure a minimum of three cycles at 3Δ before failure due to beam plastic hinging. The results have shown

that volumetric weld imperfections, at sizes much larger than specified in AS/NZS 1554.1 (AS/NZS, 2004), provide acceptable performance for the specimens investigated. With the consistent ductile nature of failure of these and other tests (Scholz, McClintock, Kiekmann, Scherer, and Nuebling, 1999; Hyland et al., 2000; Short et al., 2004), it is expected that specimens within the parameters investigated will not fail in an unacceptable and premature manner.

It has previously been mentioned that a weak panel zone may contribute to weld fracture, while the employment of a strong panel zone may be used to prevent weld fracture. All the specimens with strong to very strong panel zones reported here were shown to have enhanced performance. However, it must be reiterated that a yielding panel zone may provide additional ductile capacity to the assemblage.

Rigid backing due to an end plate or an extra strong panel zone imposes maximum inelastic demand on the beam. All specimens with strong and very strong panel zones achieved Category 1 (fully ductile) response. This performance demonstrates that a 410 UB 54 beam achieves the minimum plastic hinge rotation requirements for Category 1 (fully ductile) response with limited contribution to deformation from the panel zone. That is, the inherent deformation capacity of the beam is considered to provide acceptable deformation capacity for the connection.

If a comparison is made of the performance of specimens BE18–BE20 with BC28 and BC29, one would expect the earlier specimens to fail earlier, due to a reduction in the contribution to deformation from the support (in other words, the first assumption outlined in the design of the modified beam-end-plate connection). However, the second assumption, where the stiffness in the supports is at least as great as that in the beam-column, was shown to not hold. It is reasonable to assume that the marginally greater yield deflection is due to differences in the test configurations and subsequent strong wall reactions. Measurements of the strong wall deflection revealed that at the 3Δ step there was a ±0.5 mm difference between test configurations. The greater deflection for the end-plate specimens is explained by the nature of the bearing in the steel base plate to concrete strong wall connection. Rather than a smooth surface, the concrete strong-wall is ribbed, reflecting the pattern of the formwork into which the strong wall was poured. When the Maccalloy bars are pretensioned, the end-plate is tied into the wall. The end-plate bears against the ribs rather than against a solid concrete surface. These ribs are ≅ 3 mm high such that when the specimen is bolted into place and prior to loading there is a gap of some 2 mm between the base plate and the solid surface of the strong wall. When subjected to bending, the base plate further compresses the ribs and bears against the solid surface of the strong wall. The rotation associated with this is probably responsible for the larger than expected Δ observed experimentally.

CONCLUSION

Two limits for the failure of welded moment-resisting connections were identified from large-scale cyclic testing of fillet welded moment-resisting connections (MRCs). A worst-case volumetric imperfection and strong (nearly rigid) panel zone were determined for acceptable deformation capacity.

Volumetric imperfections in the beam flange fillet welds were shown to change the failure mode from beam plastic hinging to cyclic ductile overload of the weldment. None of the specimens tested failed with brittle fracture. Typically both modes initiated, with significant interaction evident before one mode developed to a critical size and prevailed. A volumetric imperfection simulated by an aggregate reduction in the load-bearing cross-section at the flange edge of the fillet weld by 10% was shown to produce cyclic ductile overload of the weldment. If cyclic ductile overload of the weldment is an acceptable limit state, the connection was shown to provide marginally acceptable deformation capacity. The stress concentration due to a 5% flange-edge volumetric imperfection was determined to act as a threshold between the two failure modes for the model investigated.

Strong panel zones were shown to limit the influence of the imperfection such that the welds in these connections were seen to have enhanced performance. This is because the reduction of strain in the support corresponds to a reduction of strain in the weldment. Although the welds were shown to have enhanced performance, all specimens with strong panel zones were shown to be at the threshold for acceptable deformation capacity due to increased demand on the beam material. As such, the inherent deformation capacity of the beam is considered to provide acceptable deformation capacity for the connection.

Double-sided fillet welds applied in an economic manner (in other words, to light section sizes), employing notch-tough materials and designed using the stress component approach described herein were determined to provide satisfactory seismic performance.

ACKNOWLEDGMENTS

This research was undertaken at the University of Auckland as part of a larger New Zealand Heavy Engineering Research Association (HERA) research project. Financial support was provided by the Foundation for Research, Science and Technology (FRST) under an overall program entitled "Enhanced Steel Building Performance in High Risk Events." The authors would like to acknowledge HERA staff for their assistance and Grayson Engineering Ltd., Steltech Structural Ltd., and B.A. Short Ltd. for fabrication support.

REFERENCES

AS/NZS (1995), "Structural Steel Welding Part 5: Welding of Steel Structures Subject to High Levels of Fatigue Loading," 1554.5, Homebush, Australia, Standards Australia/Standards New Zealand, pp. 51–56.

NZS 3404 (1997), "Part 1: Steel Structures Standard," Wellington, Standards New Zealand.

IIW (2003), "Recommendations for Assessment of Risk of Fracture in Seismically Affected Moment Connections," IIW-X-1504-02, IIW-XV-1102-02, pp. 1–32.

AS/NZS (2004), "Structural Steel Welding Part 1: Welding of Steel Structures," 1554.1, Wellington, New Zealand, Standards Australia/Standards New Zealand.

AS/NZS (2004), "Commentary on the Standard AS/NZS 1554 Structural Steel Welding," Lidcombe, NSW, Australia, Welding Technology Institute of Australia.

Azuma, K., Kurobane, Y., and Makino, Y. (2000), "Cyclic Testing of Beam-to-Column Connections with Weld Defects and Assessment of Safety of Numerically Modeled Connections from Brittle Fracture," *Engineering Structures*, Vol. 22, No. 12, pp. 1596–1608.

Barsom, J.M. and Pellegrino, J.V. (2002), "Failure Analysis of Welded Steel Moment-Resisting Frame Connections," *Journal of Materials in Civil Engineering*, Vol. 14, No. 1, pp. 24–34.

Calado, L., Castiglioni, C., and Bernuzzi, C. (2000), *Seismic Behaviour of Welded Beam-to-Column Joints: Experimental and Numerical Analysis*, Fourth International Workshop on Connections in Steel Structures, Roanoke, VA.

Clifton, G.C. and Butterworth, J.W. (1998), *Performance of Rigid Welded Beam-to-Column Joints Under Inelastic Cyclic Loading*, Australasian Structural Engineering Conference, Auckland.

Clifton, G.C., Weigel, M., and Rupflin, B. (1996), "Development of Moment-Resisting Steel Frames Incorporating Semi-Rigid Elastic Joints," Auckland, 1995/1996 Research Report, HERA Report R4-88.

Feeney, M.J. and Clifton, C. (1995), "R4-76: Seismic Design Procedures for Steel Structures," 1st Ed., Auckland, HERA, pp. 3.1–3.4.

Goel, S.C., Stojadinovic, B., Choi, J., and Lee. K.H. (2000), *Shear Force and Welded Steel Moment Connections*, Connections in Steel Structures IV, Roanoke, VA.

Hajjar, J.F., Dexter, R.J., Lee, D., Cotton, S.C., Ye, Y., and Ojard, S.J. (2003), "Continuity Plate Detailing for Steel Moment-Resisting Connections," *Engineering Journal*, 4th Quarter, pp. 189–211.

Hyland, C., Ferguson, G., and Butterworth, J. (2004), *Selection of Structural Steel for Seismic Performance*, New Zealand Metals Industry Conference 2004, Christchurch, HERA.

Hyland, C.W.K., Clifton, G.C., Butterworth, J.W., and Scholz, W. (2000), *Performance of Rigid Welded Beam-to-Column Connections Under Severe Seismic Conditions*, 12th World Conference on Earthquake Engineering, Auckland.

Hyland, C.W.K., Ferguson, W.G., and Butterworth. J.W. (2003), *The Effect of Monotonic Tensile Prestrain on the Charpy V-Notch Properties of AS/NZS 3679.1 G300 Structural Steel Sections,* 2003 Joint Conference of SCENZ/FEANZ/EMG, Wellington, New Zealand.

Johnson, M. (2000), *State of the Art Report on Welding and Inspection*, FEMA-355B, SAC.

Krawinkler, H. (1992), *Guidelines for Cyclic Seismic Testing of Components of Steel Structures*, ATC-24, California, Applied Technology Council, pp. 1–57.

Krawinkler, H. and Mohasseb, S. (1987), "Effects of Panel Zone Deformations on Seismic Response," *Journal of Constructional Steel Research*, Vol. 8, pp. 233–250.

Kuwamura, H. (1997), "Transition Between Fatigue and Ductile Fracture in Steel," *Journal of Structural Engineering*, Vol. 123, No. 7, pp. 864–870.

Lange, G.A. (1986), *Systematic Analysis of Technical Failures*, Verlag.

Lee, K., Goel, S.C., and Stojadinovic, B. (2000), *Boundary Effects in Steel Moment Connections*, 12th World Conference on Earthquake Engineering, Auckland, New Zealand, New Zealand Society for Earthquake Engineering.

Lu, L.-W., Ricles, J.M., Mao, C., and Fisher, J.W. (2000), "Critical Issues in Achieving Ductile Behaviour of Welded Moment Connections," *Journal of Constructional Steel Research*, Vol. 55, No. 1–3, pp. 325–341.

Mao, C.S., Ricles, J.M., Lu, L.-W., and Fisher. J.W. (2001), "Effect of Local Details on Ductility of Welded Moment Connections," *Journal of Structural Engineering,* ASCE, Vol. 127, No. 9, pp. 1036–1044.

Mohr, W. (1997), "Panel Zone Yielding as a Precursor of Brittle Fracture of Welded Connection in Special Moment-resisting Frames," *IIW Document No. X-1399-97*, *IIW Document No. XV-960-97*, pp. 118–136.

Mohr, W. (2002), "Weld Acceptance Criteria for Seismically Loaded Steel Structures," *Journal of Materials in Civil Engineering*, Vol. 14, No. 1, pp. 50–56.

NZS (1992), "General Structural Design and Design Loadings for Buildings," NZS 4203.

Phaal, R., Challenger, N.V., Maddox, S.J., and Garwood, S.J. (1995), "Current Status of Revisions to PD6493 Assessment Procedures for Fusion Welded Structures," *IIW Document No. X-1314-95*, pp. 1–14.

Plumier, A. (2000), "General Report on Local Ductility," *Journal of Constructional Steel Research*, Vol. 55, pp. 91–107.

Ricles, J.M., Mao, C., Lu L.-W., and Fisher, J.W. (2002), "Inelastic Cyclic Testing of Welded Unreinforced Moment Connections," *Journal of Structural Engineering*, Vol. 128, pp. 429–440.

Roeder, C.W. (2000), *State of the Art Report on Connection Performance*, FEMA-355D, 1, SAC: 2.

Roeder, C.W. (2002), "General Issues Influencing Connection Performance," *Journal of Structural Engineering*, Vol. 128, No. 4, pp. 420–428.

Scholz, W., McClintock, A., Diekmann, A., Scherer, J., and Nuebling, R. (1999), "Examination of Welded Moment-resisting Connections Under Low Cycle, High Strain Rate Inelastic Load," Revision March 2000, *New Zealand Welding Centre Report R8-15*, Auckland, New Zealand, HERA, pp. 1–199.

Short, A., Woerner, W., Vogele, G., and Moll, M. (2004), "Earthquake Performance of Welded Moment-resisting Connections," *New Zealand Welding Centre Report 8-28*, Auckland, New Zealand, HERA.

Stojadinovic, B. (2003), "Stability and Low-Cycle Fatigue Limits of Moment Connection Rotation Capacity," *Engineering Structures*, Vol. 25, No. 5, pp. 691–700.

Woerner, W., Mago, N., Schwarz, N., and Short, A. (2003), "Cyclic Performance of Welded Beam-to-End-Plate Connections," *New Zealand Welding Centre Report R8-23*, Auckland, New Zealand, HERA.